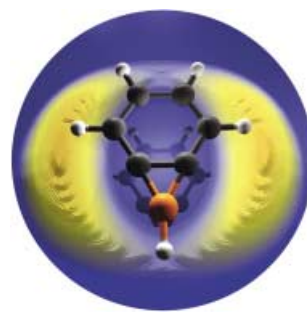


COVER PICTURE

The cover picture shows benzoborirene, the product of the crossed-molecular-beam reaction between benzene molecules and boron atoms, displayed above the three-dimensional plot of the angular- and translational-energy-dependent flux of the benzoborirene molecules in the center-of-mass system. As the reaction conditions preclude secondary collisions, the intermediate initially formed from the reactive collision decays by ejection of a hydrogen atom. The structure of the benzoborirene depicted is based on a DFT computation, which, combined with results of highly accurate coupled-cluster calculations has been used to assign the reaction product by comparing experimental and theoretical reaction energies. Details are described by R. I. Kaiser and H. F. Bettinger on p. 2350 ff.

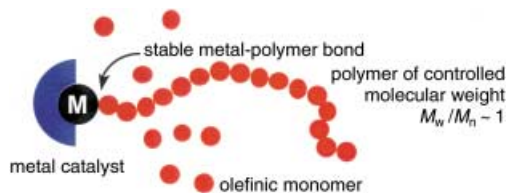


REVIEW

Contents

Polyolefins are ubiquitous materials in everyday life:

Although these polymers are traditionally synthesized by heterogeneous transition-metal catalysts, recent advances in single-site catalysts have given birth to a wide array of new materials of precise stereochemistry (see picture). Although olefin-polymerization techniques are superior to their ionic and radical counterparts regarding stereochemical control, they have been inferior in the category of living polymerization. Recent advances in alkene-polymerization catalysts are rapidly eliminating this deficit.



Angew. Chem. **2002**, *114*, 2340–2361

G. W. Coates,* P. D. Hustad,
S. Reinartz 2236–2257

Catalysts for the Living Insertion
Polymerization of Alkenes: Access to
New Polyolefin Architectures Using
Ziegler–Natta Chemistry

Keywords: alkenes • block copolymers •
homogeneous catalysis • living
polymerization • Ziegler–Natta catalysis

MINIREVIEW

The manipulation of iron uptake in plants is close to being realized. Proteins participating in iron transport have been identified and characterized in the model plant *Arabidopsis thaliana*. From this result it will be possible to engineer crop plants that take up more iron for nutritional improvement or plants that clean up toxic minerals from contaminated environments.



Angew. Chem. **2002**, *114*, 2363–2368

D. Staiger* 2259–2264

Chemical Strategies for Iron Acquisition
in Plants

Keywords: chelates • iron • reduction •
siderophores • transport proteins

HIGHLIGHTS

Improved protecting-group strategies are used in two successful methods for the synthesis of oligoribonucleotides. The effective production of these compounds is of growing importance in the context of RNA interference, a phenomenon that is exploited for investigations into protein function.

R. Micura* 2265–2269

Small Interfering RNAs and Their
Chemical Synthesis

Keywords: gene silencing • nucleic acids •
oligonucleotides • protecting groups •
RNA

Angew. Chem. **2002**, *114*, 2369–2373

The structures of AuH and AuI are already known, now the long-sought-after molecules AuH_3 ($= (\text{H}_2)\text{AuH}$) and AuH_5 ($= \text{H}_3\text{Au}(\text{H}_2)$) have been detected by matrix isolation spectroscopy. Based on new calculations, the global minimum for AuI_3 , a missing member of the gold halides, has been elucidated to be that of an L-shaped moiety (C_s symmetry; charge transfer from the I_2 unit to the AuI).

Angew. Chem. **2002**, *114*, 2373–2375

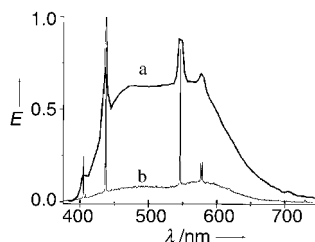
M.-J. Crawford,*
T. M. Klapötke* 2269–2271

Hydrides and Iodides of Gold

Keywords: ab initio calculations • gold • halogens • hydrides • matrix isolation

CORRESPONDENCE

Stray light is a possible source of interference in the electroluminescence spectrum of ITO/NPB/(mdppy)BF/LiF/Al reported by Wang and co-workers (see picture, trace a). Chou et al. observed that four major peaks that correspond to mercury overlap with the reported peaks (trace b).



P.-T. Chou,* C.-C. Cheng, C.-S. Chiou,
G.-R. Wu 2273

Comment on the Communication “Highly Efficient White Organic Electroluminescence from a Double-Layer Device Based on a Boron Hydroxyphenylpyridine Complex” by Wang et al.

Y. Liu, J. Guo, H. Zhang,
Y. Wang* 2274

Reply

Keywords: boron • electroluminescence • luminescence • stray light • thin films

Angew. Chem. **2002**, *114*, 2377

Angew. Chem. **2002**, *114*, 2378

VIPs

The following communications are “Very Important Papers” in the opinion of two referees. They will be published shortly (those marked with a diamond will be published in the next issue). Short summaries of these articles can be found on the *Angewandte Chemie* homepage at the address <http://www.angewandte.org>

Catalytic Activity and Poisoning of Specific Sites on Supported Metal Nanoparticles

S. Schauermaun, J. Hoffmann, V. Johánek, J. Hartmann, J. Libuda,* H.-J. Freund ◆

Understanding Zeolite Catalysis: Inverse Shape Selectivity Revised

M. Schenk, S. Calero, T. L. M. Maesen, L. L. van Benthem, M. G. Verbeek, B. Smit* ◆

Highly Selective Transport of Organic Compounds by Using Supported Liquid Membranes Based on Ionic Liquids

L. C. Branco, J. G. Crespo, C. A. M. Afonso*

Atom-Transfer Tandem Radical Cyclization Reactions Promoted by Lewis Acids

D. Yang,* S. Gu, H.-W. Zhao, N.-Y. Zhu

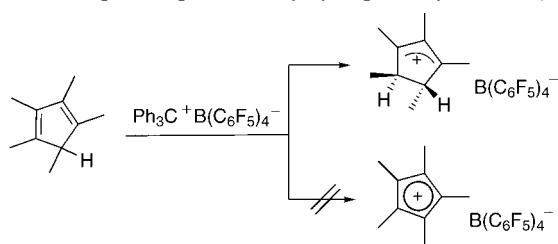
Metallabenzene and Valence Isomers: Synthesis and Characterization of a Platinabenzene

V. Jacob, T. J. R. Weakley, M. M. Haley*

Electronic and Steric Effects on Catalysts for CO_2 /Epoxide Polymerization: Extremely Subtle Modifications Resulting in Superior Activities

D. R. Moore, M. Cheng, E. B. Lobkovsky, G. W. Coates*

Not $C_5Me_5^+$ (I): $C_5Me_5^+$ remains triplet! The reaction of triphenylmethyl tetrakis(pentafluorophenyl)borate with pentamethylcyclopentadiene does not lead to a stable antiaromatic singlet pentamethylcyclopentadiene cation, but to the unexpected pentamethylcyclopentenyl cation (see scheme).



Angew. Chem. **2002**, *114*, 2379–2380

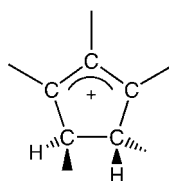
M. Otto, D. Scheschkewitz, T. Kato,
M. M. Midland, J. B. Lambert,
G. Bertrand* 2275–2276

The Stable Pentamethylcyclopentadienyl
Cation Remains Unknown

Keywords: antiaromaticity •
carbocations • cyclopentadienyl cation •
cyclopentenyl cation • structure
elucidation



Not $C_5Me_5^+$ (II): The search for the elusive singlet cyclopentadienyl cation must continue. Quantum-mechanical calculations of both structure and NMR chemical shifts suggest that the recently reported X-ray structure is that of a cyclopentenyl cation (see picture).



Angew. Chem. **2002**, *114*, 2380–2382

T. Müller* 2276–2278

Comment on the X-Ray Structure of
Pentamethylcyclopentadienyl Cation

Keywords: antiaromaticity •
carbocations • cyclopentadienyl cation •
cyclopentenyl cation • density functional
calculations • structure elucidation

Not $C_5Me_5^+$ (III): Because of the evidence presented in the above Correspondence the authors are retracting the conclusions of their publication “The Stable Pentamethylcyclopentadienyl Cation” which were entirely those of the main author and imply no reflection on the part of his co-workers (whose experimental and theoretical work is valid).

Angew. Chem. **2002**, *114*, 2383–2383

J. B. Lambert* 2279–2279

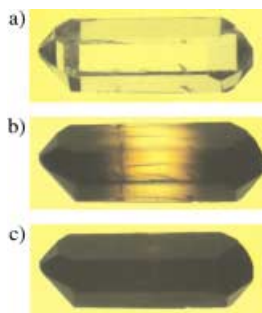
Statement

Keywords: antiaromaticity • aromaticity •
carbocations • cyclopentadienyl cation •
cyclopentenyl cation • structure
elucidation

COMMUNICATIONS

Efficient guest exchange: The organic zeolite analogue $TPP \cdot x(THF)$ ($x = 0.35–0.65$) takes up I_2 quickly when exposed to iodine vapor. The previously colorless crystals (a) color at the ends (b), and after 1–2 days the iodine has permeated all the way through the crystal (c). The conductivity values of the $TPP \cdot y(I_2)$ crystals are of the same order as those of elemental I_2 . TPP = tris(*o*-phenylenedioxy)cyclotriphosphazene.

Angew. Chem. **2002**, *114*, 2385–2388

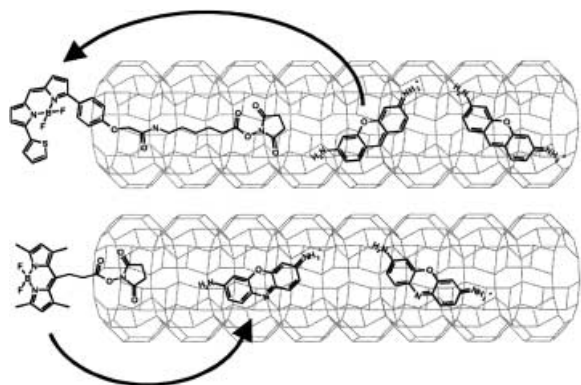


T. Hertzsch, F. Budde, E. Weber,
J. Hulliger* 2281–2284

Supramolecular-Wire Confinement of I_2
Molecules in Channels of the Organic
Zeolite Tris(*o*-phenylenedioxy)cyclo-
triphosphazene

Keywords: conducting materials •
iodine • phosphazenes • zeolite
analogues

Stopcock fluorophores at the ends of zeolite L channels can trap electronic excitation energy from pyronine⁺ molecules inside the crystal (see scheme, top). The reverse process, that is, the injection of electronic excitation energy through such stopcocks (bottom), was achieved with oxonine⁺ molecules inside the zeolite channels.



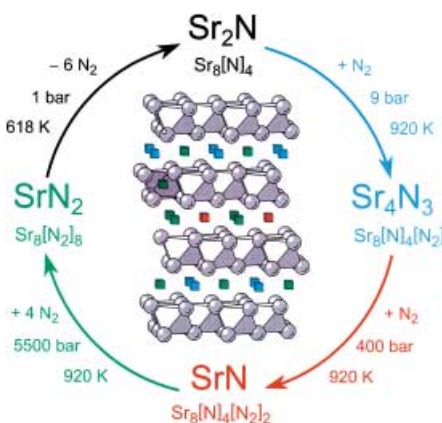
Angew. Chem. **2002**, *114*, 2389–2392

H. Maas, G. Calzaferri* 2284–2288

Trapping Energy from and Injecting Energy into Dye–Zeolite Nanoantennae

Keywords: donor–acceptor systems • dyes/pigments • fluorescence • supramolecular chemistry • zeolites

The reaction of molecular nitrogen with the layered subnitride Sr₂N leads to intercalation and formation of single-phase Sr₂N[N₂]_{0.25} (≡ Sr₄N₃; see scheme) under mild conditions (*T* = 650 °C, *p*_{N₂} = 9 bar). N₂ is reduced to the diazenide stage [N₂²⁻], while half of the strontium is oxidized to Sr²⁺. The intercalation is reversible.



Angew. Chem. **2002**, *114*, 2392–2394

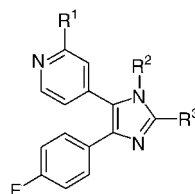
Y. Prots, G. Auffermann, M. Tovar, R. Kniep* 2288–2290

Sr₄N₃: A Hitherto Missing Member in the Nitrogen Pressure Reaction Series
Sr₂N → Sr₄N₃ → SrN → SrN₂

Keywords: diazenides • intercalation • nitrides • pressure synthesis • subvalent compounds



Regioselective synthetic approaches to tetrasubstituted imidazoles (see picture) are reported. These highly substituted heterocycles are potent inhibitors of cytokine release and therefore interesting candidates for anti-inflammatory drugs.



Angew. Chem. **2002**, *114*, 2408–2411

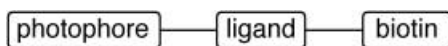
S. Laufer,* G. Wagner, D. Kotschenreuther 2290–2293

Ones, Thiones, and *N*-Oxides: An Exercise in Imidazole Chemistry

Keywords: drug design • inhibitors • medicinal chemistry • nitrogen heterocycles • synthetic methods



Two generally applicable reagents for photoaffinity probes have been developed. They contain an *m*-nitrophenyl ether function with a trifluoromethyldiazirine side chain (photophore group), as well as a biotin tag for the identification of labeled proteins or peptides and either a free hydroxy or a squaramide group for the attachment of any suitably functionalized ligand which directs the reagent to the binding site of the target molecule (see picture).



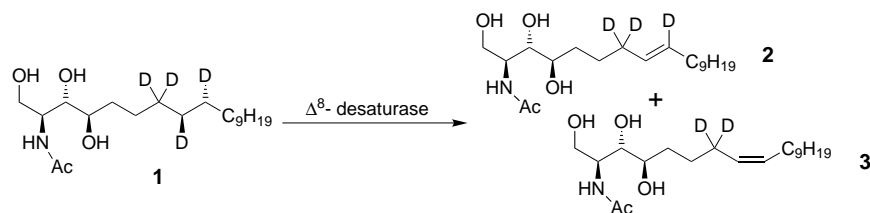
Angew. Chem. **2002**, *114*, 2404–2408

M. Daghighi, L. Hennig, M. Findeisen, S. Giesa, F. Schümer, H. Hennig, A. G. Beck-Sickinger, P. Welzel* 2293–2297

Tetrafunctional Photoaffinity Labels Based on Nakanishi's *m*-Nitroalkoxy-Substituted Phenyltrifluoromethyldiazirine

Keywords: antibiotics • photoaffinity labels • photochemistry • transglycosylase

The simultaneous formation of *E* and *Z* double bonds results from the *syn* elimination of H and/or D atoms from different conformations of 4-hydroxy-sphinganine [D₄]**1**. Δ^8 -Sphingolipid desaturase from *Helianthus annuus* is heterologously expressed in yeast and catalyzes the transformation to *E* olefin **2** (88%) and *Z* olefin **3** (12%).



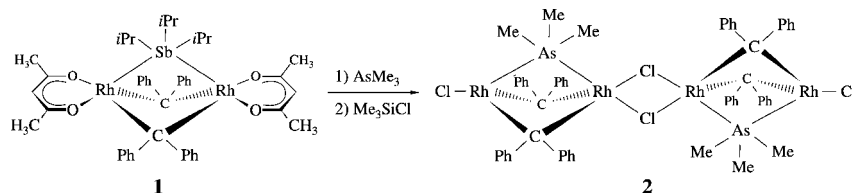
Angew. Chem. **2002**, *114*, 2394–2397

C. Beckmann, J. Rattke, N. J. Oldham,
P. Sperling, E. Heinz,
W. Boland* 2298–2300

Characterization of a Δ^8 -Sphingolipid
Desaturase from Higher Plants: A
Stereochemical and Mechanistic Study on
the Origin of *E,Z* Isomers

Keywords: desaturases • elimination •
enzyme catalysis • isotope effects •
sphingolipids

A tertiary arsane ligand in a bridging position occurs for the first time in the structurally characterized transition-metal complex **2**, which was prepared from **1** by stepwise ligand substitution of both the trialkylstibane and acetylacetonate ligands. The analogous chainlike phosphane-bridged dimer [ClRh(μ -PMe₃)(μ -CPh₂)₂Rh(μ -Cl)₂Rh(μ -PMe₃)(μ -CPh₂)₂RhCl] has also been isolated and characterized by X-ray crystallography.



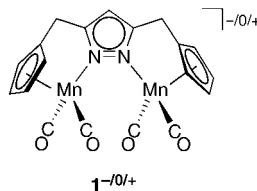
Angew. Chem. **2002**, *114*, 2398–2401

T. Pechmann, C. D. Brandt, C. Röger,
H. Werner* 2301–2303

A New Type of Chainlike Tetranuclear
Rhodium Complexes with PR₃ and AsMe₃
as Bridging Ligands

Keywords: As ligands • bridging ligands •
carbene complexes • P ligands • rhodium

Fast electron transfer between the Mn centers in the mixed-valent complex **1**, a dinuclear analogue of complexes with Cp'-N-ligands (Cp = C₅H₅), supports the occurrence of cooperative effects in such highly preorganized bimetallic systems. An unusual $\eta^1:\eta^1:\eta^5$ coordination of the pyrazolate group is observed for K⁺ **1** in the solid state.



Angew. Chem. **2002**, *114*, 2414–2417

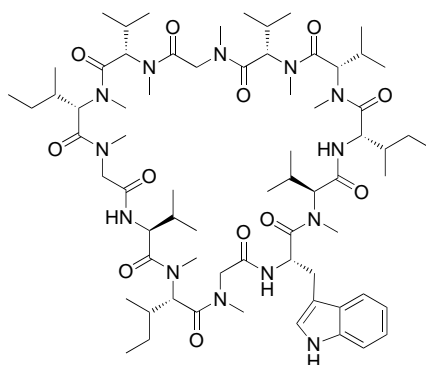
J. C. Röder, F. Meyer,*
E. Kaifer 2304–2306

Bifunctional Cp \cap N Complexes—
Unusual Structural Features and
Electronic Coupling in Highly
Preorganized Bimetallic Systems

Keywords: bridging ligands • electronic
structure • manganese • metal–metal
interactions • mixed-valent compounds



Racemization-free coupling of Fmoc-*N*-methyl amino acids on a solid support is quantitative with a new triphosgene-activation method. With this method, the total synthesis of the nematocidal cyclododecapeptide omphalotin A (see picture) was accomplished, which because of its high content of *N*-methyl amino acids had not yet been accessible.



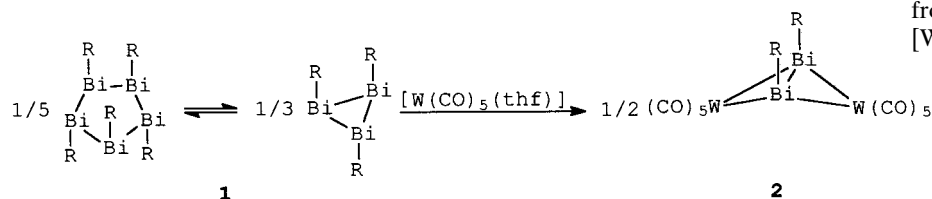
Angew. Chem. **2002**, *114*, 2401–2403

B. Thern, J. Rudolph,
G. Jung* 2307–2309

Total Synthesis of the Nematocidal
Cyclododecapeptide Omphalotin A by
Using Racemization-Free Triphosgene-
Mediated Couplings in the Solid Phase

Keywords: *N*-methyl amino acids •
omphalotin A • peptides • solid-phase
synthesis • total synthesis • triphosgene

The wings of the butterfly structure are widely extended in 2 (see picture, $R = \text{Me}_3\text{SiCH}_2$), a complex with a dibismuthene ligand, which coordinates as a “side-on”-bridging, four-electron donor to two tungsten atoms. Complex **2** is formed from the reaction of $[\text{W}(\text{CO})_5(\text{thf})]$ with alkylbismuth five- and three-membered rings of cyclobismuthanes **1**, which exist in equilibrium.



Angew. Chem. **2002**, *114*, 2411–2414

L. Balázs, H. J. Breunig,*

E. Lork 2309–2312

Synthesis of the Dibismuthene Complex
 $[\{\mu\text{-}\eta^2\text{-(cis-Me}_3\text{SiCH}_2\text{Bi)}_2\}\{\text{W}(\text{CO})_5\}_2]$
 from a Cyclobismuthane and
 $[\text{W}(\text{CO})_5(\text{thf})]$

Keywords: bismuth • small-ring systems • structure elucidation • tungsten

What's new about complexes 1 and 2, textbook examples of coordination compounds? Quantum-chemical simulations reveal an exceptionally strong sensitivity of their ^{57}Fe NMR spectroscopy chemical shifts to the Fe–C bond length, which, in turn, changes noticeably on going from the gas phase to aqueous solution.



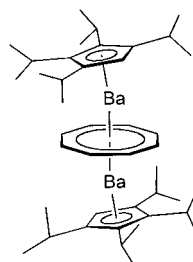
Angew. Chem. **2002**, *114*, 2417–2420

M. Bühl,* F. T. Mauschick, F. Terstegen,
 B. Wrackmeyer 2312–2315

Remarkably Large Geometry
 Dependence of ^{57}Fe NMR Chemical
 Shifts

Keywords: density functional calculations • iron • molecular dynamics • NMR spectroscopy • solvent effects

Sublimable without decomposition is the first barium triple-decker sandwich complex $[(^4\text{Cp})\text{Ba}(\text{cot})\text{Ba}(^4\text{Cp})]$ ($^4\text{Cp} = \text{C}_5\text{H}_7\text{Pr}_4$; cot = cyclooctatetraene; see picture). Short distances (significantly below the sum of Van der Waals radii) between two of the methyl groups of each ^4Cp ligand indicate a $\text{Ba} \cdots \text{CH}_3$ interaction.



Angew. Chem. **2002**, *114*, 2421–2422

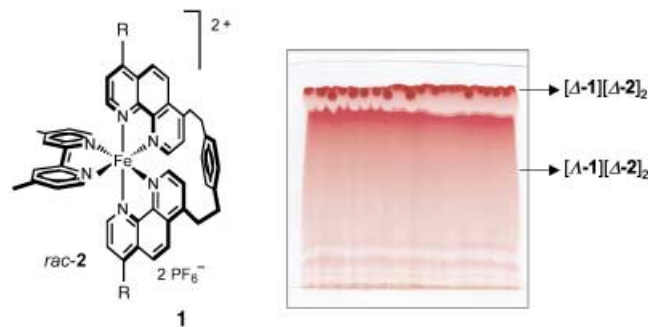
H. Sitzmann,* M. D. Walter,

G. Wolmershäuser 2315–2316

A Triple-Decker Sandwich Complex of Barium

Keywords: alkaline-earth metals • barium • cyclopentadienyl ligands • structure elucidation • triple-decker complexes

Configurational stability is conferred on the complex **1** ($R = 4\text{-MeOC}_6\text{H}_4$) by the carefully designed tetradentate bis(1,10-phenanthroline) ligand. The resolution and asymmetric synthesis of **1** were readily achieved by using tris(tetrachlorobenzenediolato)phosphate(v) anions (**2**) as chiral auxiliaries. The picture shows the separation of the enantiomers of **1** by preparative ion-pair thin-layer chromatography.



Angew. Chem. **2002**, *114*, 2423–2425

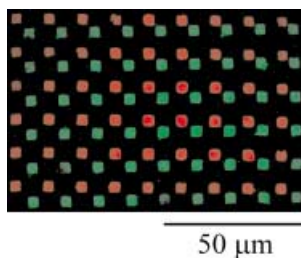
D. Monchaud, J. J. Jodry, D. Pomeranc,
 V. Heitz, J.-C. Chambron, J.-P. Sauvage,
 J. Lacour* 2317–2319

Ion-Pair-Mediated Asymmetric Synthesis
 of a Configurationally Stable
 Mononuclear Tris(diimine)–Iron(II)
 Complex

Keywords: chiral auxiliaries • chiral resolution • ion pairs • iron • N ligands



High-resolution arrays of antibodies can be prepared in a highly parallel manner by a combination of affinity purification and microcontact printing. Arrays with lateral dimensions of between 100 and 3 μm were prepared by using planar, affinity stamps that were patterned by using various soft lithographic techniques. The fluorescence microscopy image shown demonstrates the placement of anti-chicken and anti-goat antibodies on a glass substrate from a stamp.



Angew. Chem. **2002**, *114*, 2426–2429

J. P. Renault, A. Bernard, D. Juncker,
B. Michel, H. R. Bosshard,
E. Delamarche* 2320–2323

Fabricating Microarrays of Functional
Proteins Using Affinity Contact Printing

Keywords: antibodies • antigens •
lithography • microcontact printing •
patterning

A crop of gold circles and lines:

Psoralen-functionalized Au nanoparticles incorporated into DNA, and Au-nanoparticle-functionalized poly-L-lysine, yield linear and circular nanowires, respectively, on mica surfaces (see atomic force microscopy images).



Angew. Chem. **2002**, *114*, 2429–2433

F. Patolsky, Y. Weizmann,
O. Lioubashevski,
I. Willner* 2323–2327

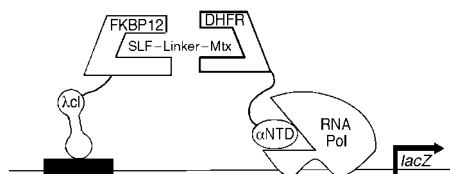
Au-Nanoparticle Nanowires Based on
DNA and Polylysine Templates

Keywords: DNA • gold • intercalation •
nanoparticles • nanostructures •
nanowires



A method for in vivo affinity chromatography,

the yeast three-hybrid assay simplifies protein identification and amplification at the end of affinity panning. The bacterial system described should increase, by several orders of magnitude, the number of protein variants that can be assayed (see picture; SLF = synthetic analogue of FK506; Mtx = methotrexate; FKBP12 = FK506-binding protein 12; DHFR = dihydrofolate reductase; λCI = λ -repressor; αNTD = N-terminal domain of the α -subunit of RNA Pol; RNA Pol = RNA polymerase).



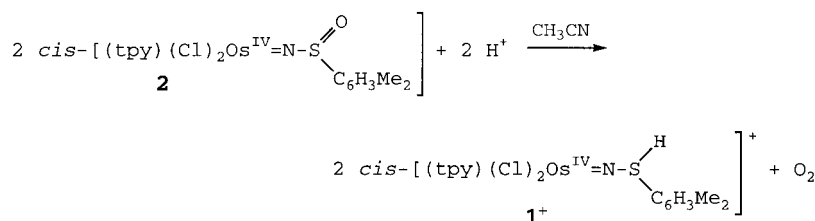
Angew. Chem. **2002**, *114*, 2433–2436

E. A. Althoff,
V. W. Cornish* 2327–2330

A Bacterial Small-Molecule Three-
Hybrid System

Keywords: bioorganic chemistry • gene
expression • protein engineering •
proteomics • signal transduction

Librating oxygen: In a novel example of O_2 evolution/activation based on a ligand, in this case, one electronically activated by the Os–N multiple bond, compound **2** ($\text{tpy} = 2,2':6',2''\text{-terpyridine}$) is converted reversibly into **1**⁺ on addition of H^+ ions. These reactions are remarkable both for their occurrence and for the rates at which they occur.



Angew. Chem. **2002**, *114*, 2436–2439

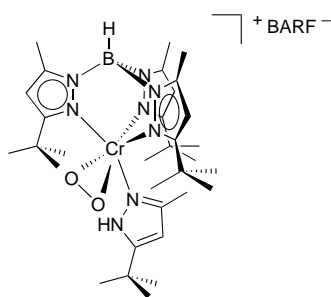
M. H. V. Huynh,* D. E. Morris,
P. S. White, T. J. Meyer* 2330–2333

Proton-Induced, Reversible Evolution of
 O_2 from the Os^{IV} –Sulfoximido Complex
[$\text{Os}^{\text{IV}}(\text{tpy})(\text{Cl})_2[\text{NS}(\text{O})\text{-}3,5\text{-Me}_2\text{C}_6\text{H}_3]$]

Keywords: N ligands • osmium • oxygen
evolution • redox chemistry • S ligands

Binding oxygen: A four-coordinate chromium(II) complex binds O_2 to yield the first structurally characterized chromium(III) superoxo complex. The superoxide ligand is coordinated in a “side-on” fashion (see structure; BARF = tetrakis(3,5-bis(trifluoromethyl)phenyl)borate). This bonding mode seems to be more widespread than commonly appreciated.

Angew. Chem. **2002**, *114*, 2439–2441



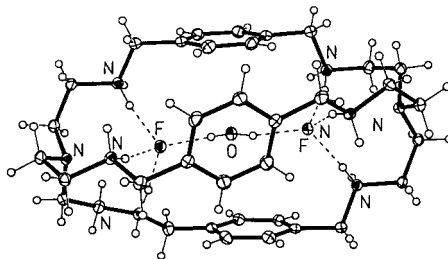
K. Qin, C. D. Incarvito, A. L. Rheingold, K. H. Theopold* 2333–2335

A Structurally Characterized Chromium(III) Superoxide Complex Features “Side-on” Bonding

Keywords: chromium • coordination modes • dioxygen • N ligands • tripodal ligands



Two fluoride ions in a single azacryptand: The two fluoride ions are bridged by a water molecule (see structure) to give an anion-based cascade complex, which mimics the analogous transition-metal cascade complexes with these ligands.



Angew. Chem. **2002**, *114*, 2441–2444

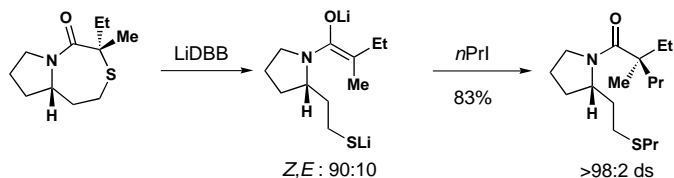
M. A. Hossain, J. M. Llinares, S. Mason, P. Morehouse, D. Powell, K. Bowman-James* 2335–2338

Parallels in Cation and Anion Coordination: A New Class of Cascade Complexes

Keywords: anions • bridging ligands • cascade complex • cryptands • macrocyclic ligands



High diastereoselectivity is achieved in the alkylation of α,α -disubstituted amide enolates to form quaternary carbon products (see scheme; LiDBB = di-*tert*-butyldiphenyllithium). No chelating groups are necessary for stereocontrol in either the enolate-formation or alkylation steps. In many cases, amplification of the alkylation diastereoselectivity above the isomeric ratio of the intermediate enolates is observed.



Angew. Chem. **2002**, *114*, 2444–2447

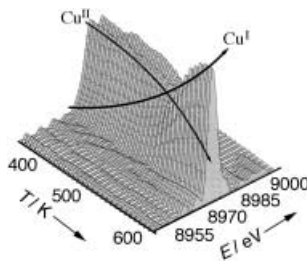
J. M. Manthorpe, J. L. Gleason* 2338–2341

Stereoselective Formation of Quaternary Carbon Centers: Alkylation of α,α -Disubstituted Amide Enolates

Keywords: alkylation • amides • asymmetric synthesis • lactams • quaternary carbon centers



The rate-determining step of the ethylene oxychlorination reaction on $CuCl_2/\gamma-Al_2O_3$ catalyst could be identified by an in situ, time-resolved XANES study. According to these data (see figure; E = photon energy) and the simultaneously determined catalyst activity, the rate-determining step is the oxidation of $CuCl$. The dopant potassium chloride, added to the industrial catalysts, decreases the rate of the reduction step, which becomes the rate-determining step for the $KCl/CuCl_2/\gamma-Al_2O_3$ catalyst.



C. Lamberti,* C. Prestipino, F. Bonino, L. Capello, S. Bordiga, G. Spoto, A. Zecchina, S. Diaz Moreno, B. Cremaschi, M. Garilli, A. Marsella, D. Carmello, S. Vidotto, G. Leofanti 2341–2344

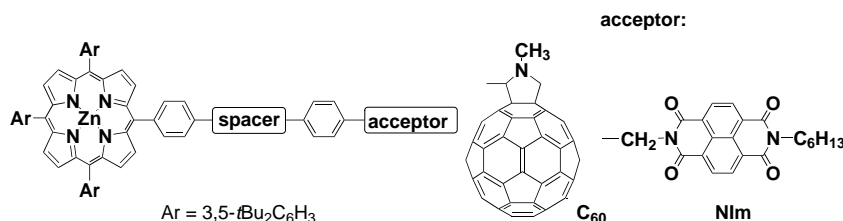
The Chemistry of the Oxychlorination Catalyst: an In Situ, Time-Resolved XANES Study

Keywords: copper • ethylene • oxychlorination • redox chemistry • X-ray absorption spectroscopy

Angew. Chem. **2002**, *114*, 2447–2450



Do electrons prefer to visit planes or spheres? Reorganization energies for intramolecular electron transfer involving a 3D acceptor (C_{60}) and a 2D acceptor (Nlm; see scheme) have been determined. Comparison of reorganization energies for the intra- versus intermolecular electron transfer has provided, for the first time, valuable insight into the intrinsic reorganization energies relating to different molecular shapes.



Angew. Chem. **2002**, *114*, 2450–2453

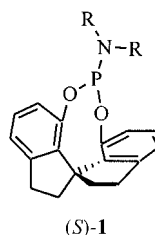
H. Imahori,* H. Yamada, D. M. Guldi,*
Y. Endo, A. Shimomura, S. Kundu,
K. Yamada, T. Okada,* Y. Sakata,
S. Fukuzumi* 2344–2347

Comparison of Reorganization Energies
for Intra- and Intermolecular Electron
Transfer

Keywords: donor–acceptor systems •
electron transfer • fullerenes •
photosynthesis • porphyrinoids



Monodentate phosphorus ligands, too, can be effective: Chiral amine derivatives can be obtained in high enantioselectivities (up to 99.7% *ee*) by the asymmetric hydrogenation of enamides in the presence of rhodium complexes of the chiral spiro phosphorus ligands (*S*)-**1**, the first monodentate P ligands that are effective in this class of reactions.



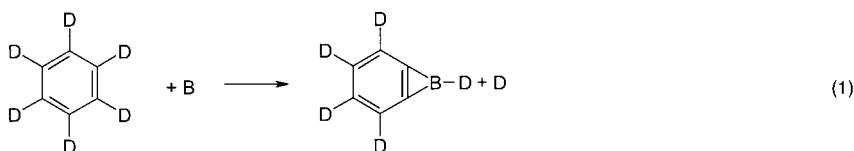
A.-G. Hu, Y. Fu, J.-H. Xie, H. Zhou,
L.-X. Wang, Q.-L. Zhou* ... 2348–2350

Monodentate Chiral Spiro
Phosphoramidites: Efficient Ligands for
Rhodium-Catalyzed Enantioselective
Hydrogenation of Enamides

Keywords: asymmetric catalysis •
homogeneous catalysis • hydrogenation •
P ligands • spiro compounds

Angew. Chem. **2002**, *114*, 2454–2456

A versatile atomic boron versus hydrogen exchange led to the formation of perdeuterated benzoborirene in the gas phase according to Equation (1). It might well be that this concept could also be adapted to form more complex heteroaromatic boron-bearing molecules in the gas phase.



Angew. Chem. **2002**, *114*, 2456–2458

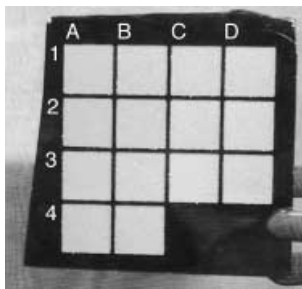
R. I. Kaiser,*
H. F. Bettinger* 2350–2352

Gas-Phase Detection of the Elusive
Benzoborirene Molecule

Keywords: ab initio calculations •
aromaticity • benzene • boron • mass
spectrometry



Scribing in the presence of reactive species enables silicon to be chemomechanically patterned and simultaneously functionalized with monolayers. Arrays of patches of monolayers are created by scribing different regions of silicon in the presence of different reagents, as shown for the homologous series of 1-alkenes from 1-pentene (A1) to 1-octadecene (B4).



T. L. Niederhauser, Y.-Y. Lua, G. Jiang,
S. D. Davis, R. Matheson, D. A. Hess,
I. A. Mowat, M. R. Linford* 2353–2356

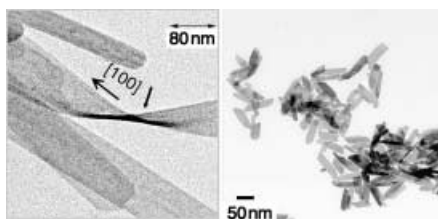
Arrays of Chemomechanically Patterned
Patches of Homogeneous and Mixed
Monolayers of 1-Alkenes and Alcohols on
Single Silicon Surfaces

Keywords: alcohols • alkenes •
monolayers • silicon • surface chemistry

Angew. Chem. **2002**, *114*, 2459–2462



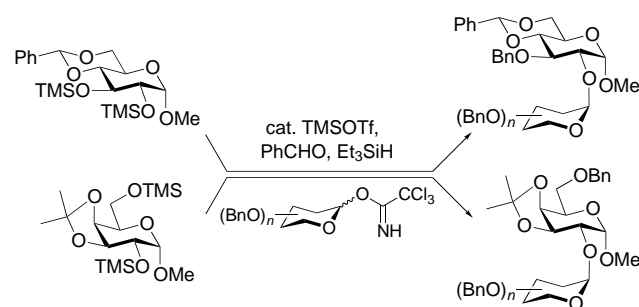
With double jets to nanobelts: Well-defined very thin CdWO_4 nanorods/nanobelts can be easily synthesized by double-jet crystallization in aqueous solution at room temperature in the absence of a polymeric crystallization modifier (see picture, left). Further hydrothermal ripening leads to the self-assembly of the nanorods/nanobelts into raftlike bundles, whereas very thin 2D sheetlike nanocrystals (see picture, right) and 1D nanorods with diameter 2.5 nm are obtained in the presence of double-hydrophilic block copolymers. Both the 1D and 2D polymer-modified species show highly increased fluorescence efficiency.



Angew. Chem. **2002**, *114*, 2462–2466



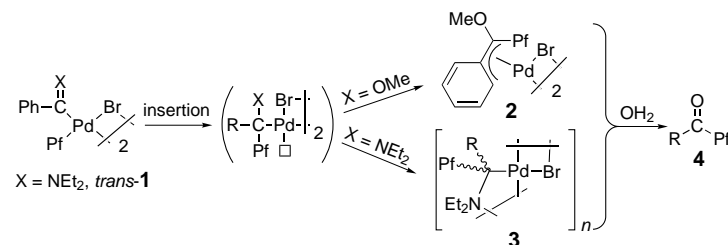
A highly regioselective benzyl and allyl protection of D-hexopyranosides allows their application in the synthesis of biologically potent $\alpha 1 \rightarrow 2$ linked disaccharide derivatives by means of a regioselective one-pot protection–glycosylation (see scheme).



Angew. Chem. **2002**, *114*, 2466–2468

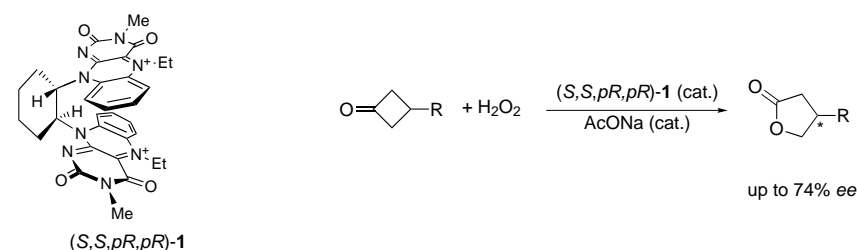


The interaction of an electrophilic carbene carbon atom with the π -electron density of an aryl group favors an intramolecular migratory insertion reaction (see scheme; $\text{Pf} = \text{C}_6\text{F}_5$). This reaction gives alkyl compounds (**2** or **3**) which can be identified prior to their eventual hydrolysis to **4**.



Angew. Chem. **2002**, *114*, 2469–2472

The chiral organocatalyst bisflavin **1** catalyzes the asymmetric Baeyer–Villiger reaction of cyclobutanones with H_2O_2 (see scheme). The corresponding lactones are obtained with up to 74% *ee*.



Angew. Chem. **2002**, *114*, 2472–2474

S.-H. Yu,* M. Antonietti, H. Cölfen,
M. Giersig 2356–2359

Synthesis of Very Thin 1D and 2D CdWO_4
Nanoparticles with Improved
Fluorescence Behavior by Polymer-
Controlled Crystallization

Keywords: block copolymers • crystal
growth • fluorescence •
morphosynthesis • nanoparticles • self-
assembly

C.-C. Wang, J.-C. Lee, S.-Y. Luo,
H.-F. Fan, C.-L. Pai, W.-C. Yang, L.-D. Lu,
S.-C. Hung* 2360–2362

Synthesis of Biologically Potent
 $\alpha 1 \rightarrow 2$ -Linked Disaccharide Derivatives
via Regioselective One-Pot Protection–
Glycosylation

Keywords: carbohydrates • glycosides •
glycosylations • oligosaccharides •
protecting groups

A. C. Albéniz,* P. Espinet,* R. Manrique,
A. Pérez-Mateo 2363–2366

Observation of the Direct Products of
Migratory Insertion in Aryl Palladium
Carbene Complexes and Their
Subsequent Hydrolysis

Keywords: carbenes • hydrolysis •
insertion • palladium • transmetalation

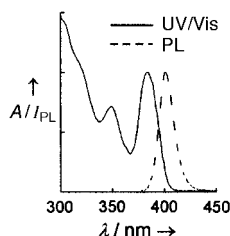
S.-I. Murahashi,* S. Ono,
Y. Imada* 2366–2368

Asymmetric Baeyer–Villiger Reaction
with Hydrogen Peroxide Catalyzed by a
Novel Planar-Chiral Bisflavin

Keywords: asymmetric catalysis •
biomimetic synthesis •
enantioselectivity • lactones • oxidation



Controllable reactivity of Cd precursors in the growth of CdS nanocrystals was achieved by varying the concentration of stabilizing ligand with a noncoordinating solvent. Such tunable reactivity is critical for developing the synthesis of semiconductor nanocrystals to the level of that of CdSe nanocrystals. The high quality of the CdS nanocrystals is indicated by the sharpness of the UV/Vis and photoluminescence spectra (see diagram, A = absorbance, I_{PL} = photoluminescence intensity).



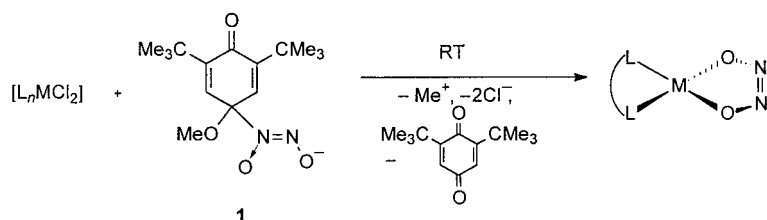
W. W. Yu, X. Peng* 2368–2371

Formation of High-Quality CdS and Other II–VI Semiconductor Nanocrystals in Noncoordinating Solvents: Tunable Reactivity of Monomers

Keywords: cadmium • nanostructures • semiconductors • solvent effects • sulfur

Angew. Chem. **2002**, *114*, 2474–2477

Ligand formed by C–N bond cleavage: Transition-metal-promoted heterolytic cleavage of the C–N bond in **1** results in the formation of five new complexes of *cis* hyponitrite with Group 10 transition metals. The new complexes include $[\text{Ni}(\eta^2\text{-O}_2\text{N}_2)(\text{dppf})]$ (dppf = 1,1'-bis(diphenylphosphanyl)ferrocene) which is structurally characterized and the thermal decomposition of which follows unimolecular kinetics.



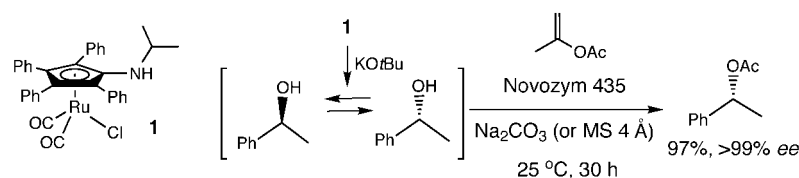
Angew. Chem. **2002**, *114*, 2477–2479

N. Arulsamy, D. S. Bohle,* J. A. Imonigie, S. Levine 2371–2373

An Umpolung Approach to *cis*-Hyponitrite Complexes

Keywords: nickel • nitrogen oxides • O ligands • P ligands • umpolung

Ruthenium–enzyme tandem catalysis: The novel racemization catalyst **1** improves the dynamic kinetic resolution (DKR) of secondary alcohols dramatically. The DKR proceeds at room temperature with isopropenyl acetate as an acyl donor. In addition, the DKR is faster even with much less lipase than in previous DKRs.



Angew. Chem. **2002**, *114*, 2479–2482

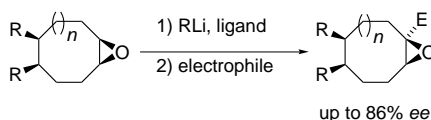
J. H. Choi, Y. H. Kim, S. H. Nam, S. T. Shin, M.-J. Kim,* J. Park* 2373–2376

Aminocyclopentadienyl Ruthenium Chloride: Catalytic Racemization and Dynamic Kinetic Resolution of Alcohols at Ambient Temperature

Keywords: asymmetric synthesis • homogeneous catalysis • kinetic resolution • lipases • ruthenium



Simple *meso*-epoxides can be asymmetrically functionalized: Ligand-assisted direct hydrogen–lithium exchange allows the generation of destabilized oxiranyl lithium species and their subsequent trapping by a wide array of electrophiles (see scheme; E = group formed by addition of electrophile). When carried out in the presence of (–)-sparteine as ligand, this reaction provides a new enantioselective route to epoxides.



D. M. Hodgson,* E. Gras ... 2376–2378

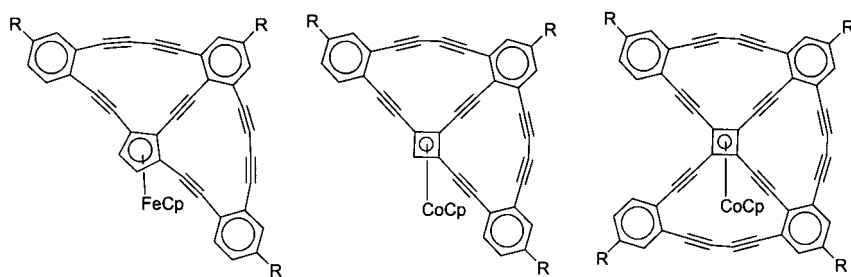
Chiral Epoxides by Desymmetrizing Deprotonation of *meso*-Epoxides

Keywords: asymmetric synthesis • carbanions • epoxides • lithiation

Angew. Chem. **2002**, *114*, 2482–2484



A combination of Pd- and Cu-catalyzed couplings make the half-wheels (see left and middle picture; Cp = C₅H₅) and the seco-wheel (right) shown here accessible. Single-crystal structures of all three target molecules have been obtained.



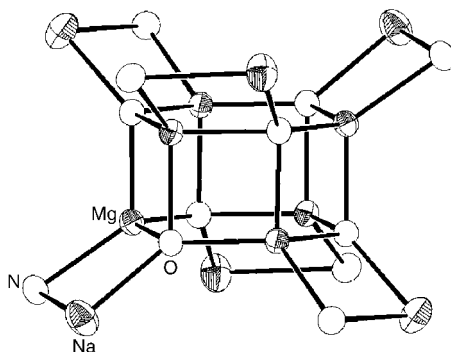
Angew. Chem. **2002**, *114*, 2484–2488

M. Laskoski, W. Steffen, J. G. M. Morton,
M. D. Smith, U. H. F. Bunz* 2378–2382

Synthesis and Structural Characterization
of Organometallic Cyclynes: Novel
Nanoscale, Carbon-Rich Topologies

Keywords: alkynes • copper •
cyclobutadiene complexes •
homogeneous catalysis • palladium

Introducing THF to synergic sodium–magnesium amide mixtures (3 tmpH:1 *n*BuNa:1 Bu₂Mg in a hydrocarbon solution; tmpH = 2,2,6,6-tetramethylpiperidine) has a surprising outcome: it leads to the cleavage of the ether and the formation of S₆-symmetric molecules with (Mg₆O₆·(NaN)₆) cores (see picture).



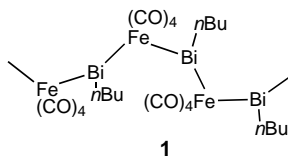
Angew. Chem. **2002**, *114*, 2488–2490

A. M. Drummond, L. T. Gibson,
A. R. Kennedy, R. E. Mulvey,*
C. T. O'Hara, R. B. Rowlings,
T. Weightman 2382–2384

Hexameric Mg–O Stacks with Six THF-
Solvated Sodium Amide Appendages:
“Super” Variants of Inverse Crown Ethers
Generated by Cleavage of THF

Keywords: alkali metals • alkaline-earth
metals • amides • cleavage reactions •
crown compounds

A unique zigzag ...-Bi-Fe-... chain forms the basis of the structure of [*n*BuBiFe(CO)₄]_∞ (**1**; see picture), which was characterized by single-crystal X-ray diffraction. Compound **1** was isolated from the ultrasonication of the dimeric product [{*n*BuBiFe(CO)₄]₂] from the reaction of [Et₄N]₃[Bi{Fe(CO)₄]₄] with *n*BuBr followed by acidification with HOAc.



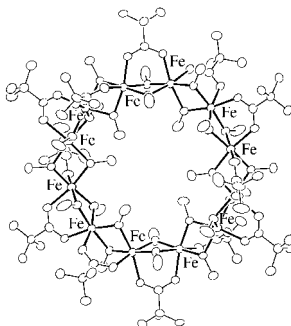
Angew. Chem. **2002**, *114*, 2490–2492

M. Shieh,* Y. Liou, M.-H. Hsu,
R.-T. Chen, S.-J. Yeh, S.-M. Peng,
G.-H. Lee 2384–2386

A Unique Bismuth–Iron Chain Polymer
Containing the ...-Bi-Fe-... Link:
Formation and Structure of
[*n*BuBiFe(CO)₄]_∞

Keywords: bismuth • carbonyl ligands •
iron • metal–metal interactions •
polymers

New wheels: The 1:2 reaction of ferric nitrate with benzoic acid (Ph₂C(OH)COOH) in methanol at pH ≈ 4.0 results in the formation of a new member of the molecular ferric-wheels family with the carboxylatobis(alkoxo) bridging unit. The molecular structure of [{Fe(OMe)₂(Ph₂C(OH)COO)]₁₂] (see picture) consists of a centrosymmetric ring of 12 Fe^{III} atoms held together by 24 μ₂-methoxide ligands and 12 1,3-bridging carboxylate ligands. The 12 metal ions are nearly coplanar and the ring size is ≈ 11.4 Å. The Mössbauer spectrum and magnetic susceptibility measurements are presented.



Angew. Chem. **2002**, *114*, 2492–2495

C. P. Raptopoulou,* V. Tangoulis,
E. Devlin 2386–2389

[{Fe(OMe)₂(O₂CC(OH)Ph₂)]₁₂:
Synthesis and Characterization of a New
Member in the Family of Molecular Ferric
Wheels with the Carboxylatobis(alkoxo)
Bridging Unit

Keywords: cluster compounds • ferric
wheels • iron • magnetic properties •
O ligands



An unprecedented yellow polymer

with low-coordinate phosphorus atoms in the backbone has been prepared. The material is soluble in polar organic solvents, and moderate molecular weights ($M_n = 2900 - 10\,500 \text{ g mol}^{-1}$) were estimated from ^{31}P NMR spectroscopic end-group analysis. The possible π -conjugation was investigated by UV/Vis spectroscopy, which revealed a red shift in λ_{max} for the polymer when compared with colorless molecular-model systems (see picture; left: model system, right: new polymer, in THF).



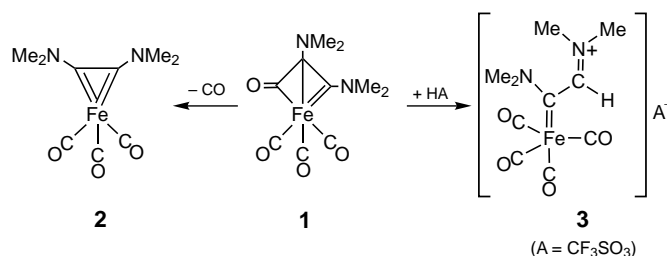
Angew. Chem. **2002**, *114*, 2495–2498

V. A. Wright, D. P. Gates* 2389–2392

Poly(*p*-phenylenephosphaalkene):
A π -Conjugated Macromolecule
Containing P=C Bonds in the Main Chain

Keywords: conjugation •
phosphaalkenes • phosphorus •
polymers • silicon

Intermediate isolated? The reaction of $[\text{Fe}(\text{CO})_5]$ with $\text{Me}_2\text{N}-\text{C}\equiv\text{C}-\text{NMe}_2$ follows an unprecedented associative pathway to give the ferrabicyclobutenone **1**. Complexes such as **1** could be key intermediates in the iron-mediated cyclization of alkynes to cyclopentadienones. Compound **1** undergoes a variety of C–C coupling and C–C-bond-cleavage reactions to afford a multitude of new organoiron compounds including **2** and **3**.



Angew. Chem. **2002**, *114*, 2499–2502

A. C. Filippou,*

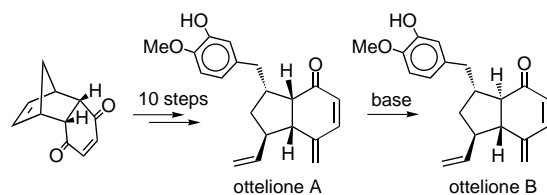
T. Rosenauer 2393–2396

A Reaction Pathway of $[\text{Fe}(\text{CO})_5]$ with
Alkynes via Ferrabicyclobutenones

Keywords: alkyne ligands • carbene
ligands • C–C coupling • iron •
metallacycles



The biologically potent antitubercular and anticancer otteliones A and B (see scheme) have been synthesized from readily available starting materials by using a short, simple, efficient, and flexible strategy. The structural ambiguity of the natural products has been resolved.



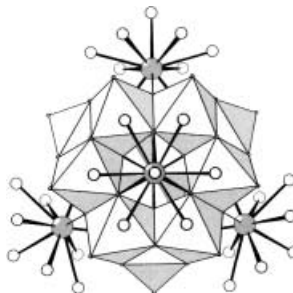
Angew. Chem. **2002**, *114*, 2502–2504

G. Mehta,* K. Islam 2396–2398

Total Synthesis of (\pm)-Otteliones A and B

Keywords: antitumor agents •
configuration determination • natural
products • total synthesis

Six Mo dimers arranged around a central PO_4 tetrahedron form the core of the novel ϵ -Keggin polyoxocation $[\epsilon\text{-PMo}_{12}\text{O}_{36}(\text{OH})_4\{\text{La}(\text{H}_2\text{O})_4\}_4]^{5+}$ (see structure) capped with four $\{\text{La}(\text{H}_2\text{O})_4\}^{3+}$ units. A ^{31}P NMR spectroscopy study shows that the ϵ -Keggin ion is unstable in aqueous solution, and leads to the formation of a polyanion/polycation salt, which is crystallographically characterized.



Angew. Chem. **2002**, *114*, 2504–2507

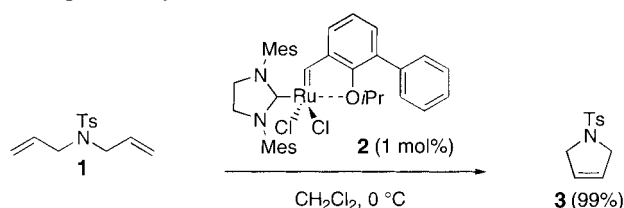
P. Mialane, A. Dolbecq, L. Lisnard,
A. Mallard, J. Marrot,
F. Sécheresse* 2398–2401

$[\epsilon\text{-PMo}_{12}\text{O}_{36}(\text{OH})_4\{\text{La}(\text{H}_2\text{O})_4\}_4]^{5+}$: The
First $\epsilon\text{-PMo}_{12}\text{O}_{40}$ Keggin Ion and Its
Association with the Two-Electron-
Reduced $\alpha\text{-PMo}_{12}\text{O}_{40}$ Isomer

Keywords: Keggin ions • lanthanum •
molybdenum • polyoxometalates • solid-
state structures



Olefin metathesis even at 0 °C! A phenyl substituent in the ruthenium catalyst **2** leads to greatly increased initiation rates in different metathesis reactions, for example, the cyclization of **1** to form **3**.



Angew. Chem. **2002**, *114*, 2509–2511

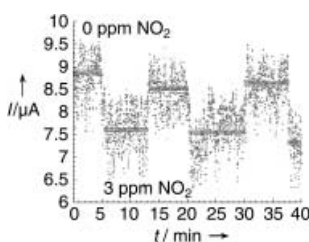
H. Wakamatsu, S. Blechert* 2403–2405

A New Highly Efficient Ruthenium Metathesis Catalyst

Keywords: homogeneous catalysis • metathesis • olefins • ruthenium



Good candidates for miniaturized, ultrasensitive gas sensors in many applications are individual single-crystalline SnO₂ nanoribbons. Here it is shown that they can be used to detect ppm-level concentrations of NO₂ at room temperature under UV illumination. The picture illustrates that they work reliably even near their resolution limit under 365-nm light.



Angew. Chem. **2002**, *114*, 2511–2514

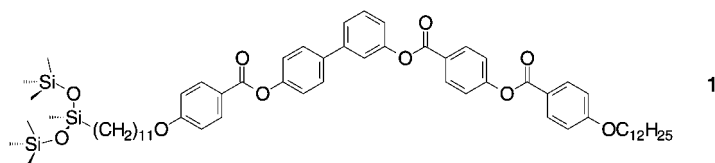
M. Law, H. Kind, B. Messer, F. Kim, P. Yang* 2405–2408

Photochemical Sensing of NO₂ with SnO₂ Nanoribbon Nanosensors at Room Temperature

Keywords: nanoribbons • nanostructures • nanowires • nitrogen dioxide • sensors



In conventional fluids the molecular dipole moments of the individual molecules cancel out, which leads to a macroscopic apolar structure. Directed molecular design using microsegregation and tailoring the molecular shape of compounds such as **1**, can lead to fluid layer structures with a macroscopic polar order.



Angew. Chem. **2002**, *114*, 2514–2518

G. Dantlgraber, A. Eremin, S. Diele, A. Hauser, H. Kresse, G. Pelzl, C. Tschierske* 2408–2412

Chirality and Macroscopic Polar Order in a Ferroelectric Smectic Liquid-Crystalline Phase Formed by Achiral Polyphilic Bent-Core Molecules

Keywords: chirality • ferroelectricity • liquid crystals • mesophases • microsegregation • siloxanes



Supporting information on the WWW (see article for access details).

* Author to whom correspondence should be addressed



Accelerated publications



BOOKS

Coffee Flavor Chemistry	Ivon Flament	<i>U. H. Engelhardt</i>	2413
Structure and Bonding in Crystalline Materials	Gregory S. Rohrer	<i>P. Kroll</i>	2413
Glycochemistry	Peng G. Wang, Carolyn R. Bertozzi	<i>T. Ziegler</i>	2414
Computational Methods in Physics, Chemistry and Biology	Paul Harrison	<i>W. Koch</i>	2416
Handbook of Modern Pharmaceutical Analysis	Satinder Ahuja, Stephen Scypinski	<i>P. Surmann</i>	2416
Object-Oriented Magnetic Resonance	Michael Mehring, Volker A. Weberruß	<i>B. Reif</i>	2417



WEB SITES

http://www.pbglinks.com	Linking Photonic Band Gaps	<i>S. Yang</i>	2419
---	-------------------------------	----------------------	------

SERVICE

• VIPs	2213	• Keywords	2420
• <i>Angewandte's</i> Sister-Journals	2229–2231	• Authors	2421
• Vacancies	A59	• Preview	2422
• Sources	A57		

Don't forget all the Tables of Contents
from 1998 onwards may be still found
on the WWW under:
<http://www.angewandte.org>

Issue 12, 2002 was published online on June 13.

APOLOGY

In the Communication “Strongly Acidic and High-Temperature Hydrothermally Stable Mesoporous Aluminosilicates with Ordered Hexagonal Structure” (Z. Zhang, Y. Han, L. Zhu, R. Wang, Y. Yu, S. Qiu, D. Zhao, F.-S. Xiao, *Angew. Chem. Int. Ed.* **2001**, *40*, 1258–1362) the thematically related manuscript “Mesoporous Aluminosilicates with Ordered Hexagonal Structure, Strong Acidity, and Extraordinary Hydrothermal Stability at High Temperatures” (Z. Zhang, Y. Han, F.-S. Xiao, S. Qiu, L. Zhu, R. Wang, Y. Yu, Z. Zhang, B. Zou, Y. Wang, H. Sun, D. Zhao, Y. Wei, *J. Am. Chem. Soc.* **2001**, *123*, 5014–5021) was not cited (and vice versa), although both manuscripts were submitted to the respective journals at the same time. The authors apologize for this mistake.

In the Minireview by **P. Cintas** in issue 7, **2002**, pp. 1139–1145, the second paragraph on the right column of page 1142 may mislead some readers, as it suggests that heterochiral peptides are unable to form a helical arrangement. In fact, previous publications (see last paragraph and ref. 52 in ref. [1]) have shown that D,L peptides are capable of forming helical structures, and this fact may be of importance for understanding the development of homochirality starting from heterochiral sequences. The chiral amplification that results from the majority rule (see ref. 40 in ref. [1]) may be large enough for a small excess of majority units to initiate the epimerization of the minority units (L) to the configuration of the majority units (D). Overall, this process, after repetitive cycles, would lead to a preferential helical sense in which the predominant chirality (D) of the units that form the polypeptides is prevalent.^[1,2] This commentary should clarify the discussion of this point in the light of past and recent literature.

[1] M. M. Green, J.-W. Park, T. Sato, A. Teramoto, S. Lifson, R. L. B. Selinger, J. V. Selinger, *Angew. Chem.* **1999**, *111*, 3329–3345; *Angew. Chem. Int. Ed.* **1999**, *38*, 3138–3154.

[2] M. M. Green, J. V. Selinger, *Science* **1998**, *282*, 879.

In the Communication by C. C. Hughes and D. Trauner in Issue 9, **2002**, pp. 1569–1572, the structures of frondosin A and frondosin B were inadvertently exchanged in Scheme 1. The numbering in Scheme 4 was also incorrect: the corrected Scheme is shown below. The editors apologize for these errors.

